units/ml penicillin G, and 100 μg/ml streptomycin, as described (29). Cultured bones were stained with Alcian blue and alizarin red dyes according to a standard protocol for skeletal preparation. Briefly, bones fixed in 96% ethanol were stained with 0.015% Alcian blue 8GX (Sigma) in a mixture solution of 96% ethanol, acetic acid (4:1) for 1 day, followed by a dehydration step in 100% ethanol. Dehydrated bones were immersed briefly in 1% potassium hydroxide (KOH), followed by staining in 0.001% alizarin red S (Sigma) in 1% KOH for 1 day. Images were analyzed using ImageJ software (National Institutes of Health). Animal experiments were approved by the Institutional Animal Care and Use Committee of Kagoshima University (MD11019).

RNA Interference—Dharmacon siRNA ON-TARGETplus SMARTpool, a mixture of four independent siRNAs of mouse SnoN (*Skil*), and the control reagent were purchased from Thermo Scientific. siRNA was transfected into cells using Lipofectamine RNAiMax (Invitrogen). Ligands and SB431542 were added to the culture simultaneously after an overnight transfection of siRNA.

Plasmids—9xCAGA luc, BRE luc, ALK5TD, ALK3QD, and FLAG-tagged human SnoN in pcDEF3 were kind gifts from Dr. Kohei Miyazono (University of Tokyo). pGL4.75hRlucCMV was purchased from Promega. cDNA of mouse SnoN was cloned from ATDC5 by employing a reverse transcription-polymerase chain reaction (RT-PCR)-based technique, subcloned into the entry vector, pENTR, and further transferred into pEF-DEST51 by attL-attR (LR) recombination (Invitrogen).

Lentivirus—pENTR-SnoN and pENTR-5′EF1αP were subjected to LR recombination with pLenti6.4/R4R2/V5-DEST (Invitrogen) to generate a lentiviral vector, which expresses C-terminal V5-tagged *SnoN* from the EF1α promoter. The lentiviral expression vector or pLenti6/V5/GW-lacZ control vector was transfected into 293FT cells to generate lentivirus. The conditioned medium containing lentivirus was incubated with mouse metatarsal bones for 16 h for infection. The infection efficiency was monitored by immunohistochemistry on the coronal section of infected bones using anti-V5-FITC antibody.

Immunoblotting—Cells were lysed in either M-PER lysis buffer (Thermo Scientific) supplemented with aprotinin, sodium orthovanadate, and phenylmethylsulfonyl fluoride (PMSF) or directly with 1× SDS sample buffer. SDS-PAGE, membrane transfer, and chemiluminescence were performed by using a standard protocol. Blots were incubated with anti-SnoN (1:200, H-317, sc-9142, Santa Cruz Biotechnology, Inc. (Santa Cruz, CA)), anti-phospho-Smad1/5/8 (1:1000, catalog no. 9511), anti-phospho-Smad2 (1:1000, catalog no. 3108), anti-Smad1 (1:1000, catalog no. 9743), horseradish peroxidase (HRP)-conjugated anti-rabbit secondary antibody and anti-mouse secondary antibody (1:10,000) (Cell Signaling), anti-Smad2/3 (1:1000, catalog no. 610842, BD Biosciences), anti-tubulin (1:1000, DM1A, T9026, Sigma), and anti-Mmp13 (1:1000, ab58836, Abcam). Signals were detected using the LAS 4000 mini image analyzer (Fujifilm).

Immunocytochemistry and Immunohistochemistry—For immunocytochemistry, cells were fixed with 4% paraformaldehyde in PBS for 30 min and treated with 0.2% Triton X-100. For antigen retrieval of type X collagen, cells were digested with 5 units/ml hyaluronidase (Calbiochem) for 30 min at 37 °C, followed by pepsin (Quartett) digestion for 15 min at 37 °C. CAS block (Zymed Laboratories Inc.) was used for blocking. Cells were incubated with anti-type X collagen (1:50, LB-0092, LSL), anti-SnoN (1:50, H-317, sc-9142, Santa Cruz Biotechnology, Inc.), anti-phospho-Smad2 (1:100, catalog no. 3108, Cell Signaling), and anti-Smad2/3 (1:100, catalog no. 610842, BD Biosciences). Anti-rabbit Alexa Fluor 488 (1:200, A11008), or anti-mouse Alexa Fluor 546 (1:200, A11060) (Invitrogen) was used to detect signals. Normal rabbit or mouse serum was used as negative control. For immunohistochemistry, we obtained human samples from individuals undergoing total hip arthroplasty after obtaining written informed consent as approved by the Ethics Committee of Kagoshima University (number 22-85). Formalin-fixed human femoral heads, mouse E17.5 embryo humeri, or bone organ culture were embedded in paraffin blocks, which were sliced at 4-μm thickness. The antigen was retrieved by using L.A.B. (Liberate Antibody Binding) solution (Polysciences), except in the case of type X collagen antigen retrieval with hyaluronidase digestion. CAS block was used for blocking except for the cultured bones, which were blocked by using 5% bovine serum albumin in PBS. Blocked sections were incubated with anti-type X collagen (1:50, LB-0092, LSL), anti-TGF-β1 (1:50, sc146, Santa Cruz Biotechnology, Inc.), anti-phospho-Smad2 (1:100, catalog no. 3103, Cell Signaling), anti-phospho-Smad3 (1:500, catalog no. 600-401-919, Rockland), anti-Smad2/3 (1:100, catalog no. 610842, BD Biosciences), anti-SnoN (1:50, H-317, sc-9142, Santa Cruz Biotechnology, Inc.), and anti-V5-FITC (1:50, R963-25, Invitrogen). Signals were detected using the REAL EnVision detecting system with DAB chromogen (Dako), anti-rabbit Alexa Fluor 488 (1:200, A11008), or anti-mouse Alexa Fluor 546 (1:200, A11060) (Invitrogen).

Real-time Quantitative PCR Assay—Cells were lysed with the TRIzol reagent (Invitrogen) to purify RNA, and 1 μg of RNA was reverse transcribed into cDNA by using the Verso cDNA Kit (Thermo Scientific). The relative amount of gene transcripts was determined by real-time PCR using the THUNDER-BIRD quantitative PCR (qPCR) mix (Toyobo) on the Thermal Cycler Dice TP850 (Takara). PCRs were performed in duplicate, and the measured expression level of each gene was normalized to that of *Hprt1*. Sequence information of primers used is listed in supplemental Table 1.
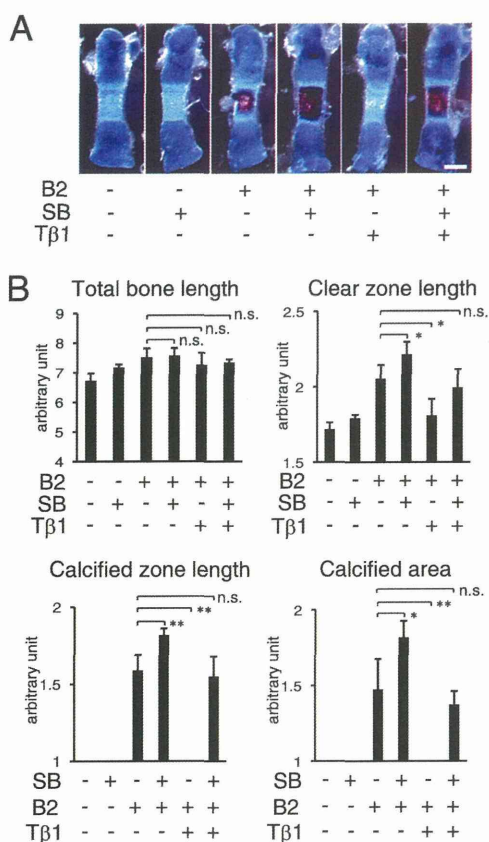
Luciferase Assay—COS-7 cells were seeded in triplicate in 24-well plates and transiently transfected with firefly reporter constructs, pGL4.75hRlucCMV *Renilla* vector, constitutively active type I receptor constructs, and the SnoN vector. Dual luciferase assays were performed as described (30) using the GloMax 96 microplate luminometer (Promega).

Statistical Analysis—Data in this study are expressed as the mean ± S.D. of at least three independent experiments. A p value of <0.05, which was determined by Student's t test, was accepted as statistically significant.
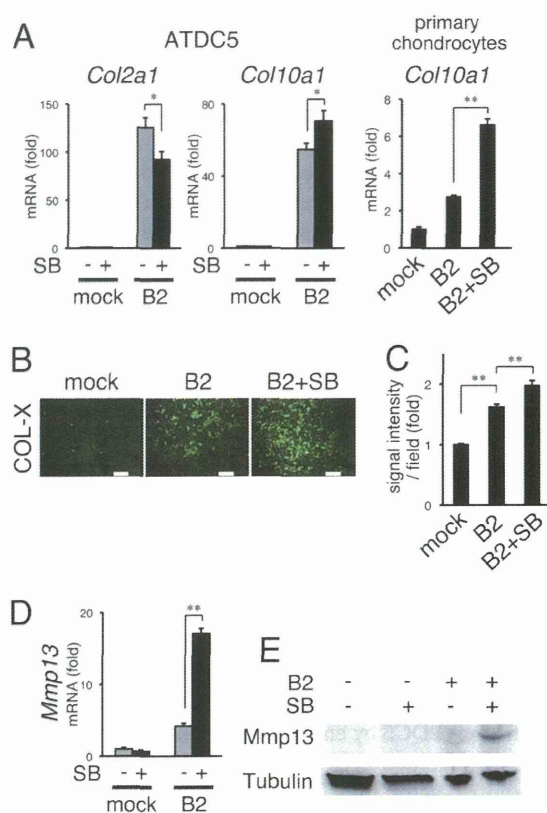
RESULTS

Endogenous TGF-β Signaling Suppresses Terminal Chondrocyte Maturation in Bone—To identify physiologically active target genes of TGF-β signaling in chondrocytes, we employed

FIGURE 1. **Endogenous TGF-β signaling prevents maturation of chondrocytes in bone organ culture.** Metatarsal bones from E17.5 mouse embryo were cultured with BMP-2 (*B2*; 300 ng/ml) or TGF-β1 (*Tβ1*; 5 ng/ml) in combination with SB431542 (*SB*; 1 μM) for 4 days. *A*, cartilage matrix was stained with Alcian blue, whereas chondrocyte matrix calcified by mature hypertrophic chondrocytes was stained by alizarin red. The clear zone represented hypertrophic chondrocytes. *B*, total bone length, clear zone length, calcified zone length, and calcified area, were analyzed on images using ImageJ software ($n = 4$). *, $p < 0.05$; **, $p < 0.01$; *n.s.*, not significant. *Error bars*, S.D.


FIGURE 2. **Loss of TGF-β signaling promotes hypertrophic conversion of chondrocytes.** *A*, expression of *Col2a1* and *Col10a1* in ATDC5 chondrocytes and mouse primary chondrocytes was analyzed by qPCR. Cells were treated with or without BMP-2 (*B2*; 300 ng/ml) in combination with SB431542 (*SB*; 1 μM). ATDC5 cells were harvested at day 5, whereas primary chondrocytes were harvested at day 14. *B* and *C*, immunocytochemistry for type X collagen (*COL-X*) was performed on micromass cultures of ATDC5 cells at day 10. *Scale bars*, 200 μm. The fluorescent signal of immunocytochemistry was quantified by ImageJ software for four independent fields per group (*C*). *D*, expression of *Mmp13* mRNA was evaluated by qPCR. *E*, expression of Mmp13 protein in ATDC5 cells at day 18 was assessed by immunoblotting. Tubulin served as a loading control. *, $p < 0.05$; **, $p < 0.01$. *Error bars*, S.D.

a TGF-β type I receptor kinase inhibitor, SB431542, to block endogenous TGF-β signaling. First, we evaluated if SB431542 could accelerate chondrocyte hypertrophy and, subsequently, matrix calcification in mouse embryonic metatarsal bone organ cultures, which is a system that allows for the study of complex chondrogenic processes in a three-dimensional structure in the context of native cell-cell and cell-extracellular matrix interactions and cellular signaling (29). The cartilage matrix was stained by Alcian blue, whereas the matrix calcified by mature hypertrophic chondrocytes was stained by alizarin red; the clear zone represented uncalcified hypertrophic chondrocytes (Fig. 1*A*). Upon treatment with BMP-2, matrix calcification was induced, whereas coapplication of TGF-β1 prevented the chondrocyte maturation. Blocking of endogenous TGF-β signaling by SB431542 in BMP-treated bone significantly enhanced the length of the clear zone as well as both length and area of the calcified matrix of cartilage; this effect was diminished by exogenous TGF-β1 application (Fig. 1, *A* and *B*). The longitudinal bone growth was slightly promoted by BMP-2, whereas SB431542 or TGF-β1 showed no effect. These results confirmed the inhibitory action of endogenous TGF-β signal-

ing in chondrocyte hypertrophy and maturation in bone rudiments.

Next, to investigate cell-autonomous actions of endogenous TGF-β signaling in BMP-induced maturation of chondrocytes, we applied SB431542 in a chondrocyte micromass culture, which is a system widely employed to study the multiple steps of cartilage differentiation (31). Upon treatment with BMP-2 in the presence of insulin/transferrin/selenium supplements, expression of *Col2a1* and *Col10a1* was induced in ATDC5 cells, as reported previously (32), whereas combined application of SB431542 mildly suppressed the level of *Col2a1* mRNA, suggesting the promotive role of TGF-β signaling in early chondrogenesis (Fig. 2*A*). In contrast, BMP-induced expression of *Col10a1* was further enhanced by SB431542 in ATDC5 cells as well as dramatically enhanced in mouse primary chondrocytes (Fig. 2*A*). Whereas treatment with BMP-2 accelerated the production of the type X collagen protein (encoded by *Col10a1*) in ATDC5 cells, SB431542 further strengthened the signal (Fig. 2*B*). The fluorescent signal of immunocytochemistry against type X collagen was significantly increased by SB431542 treat-
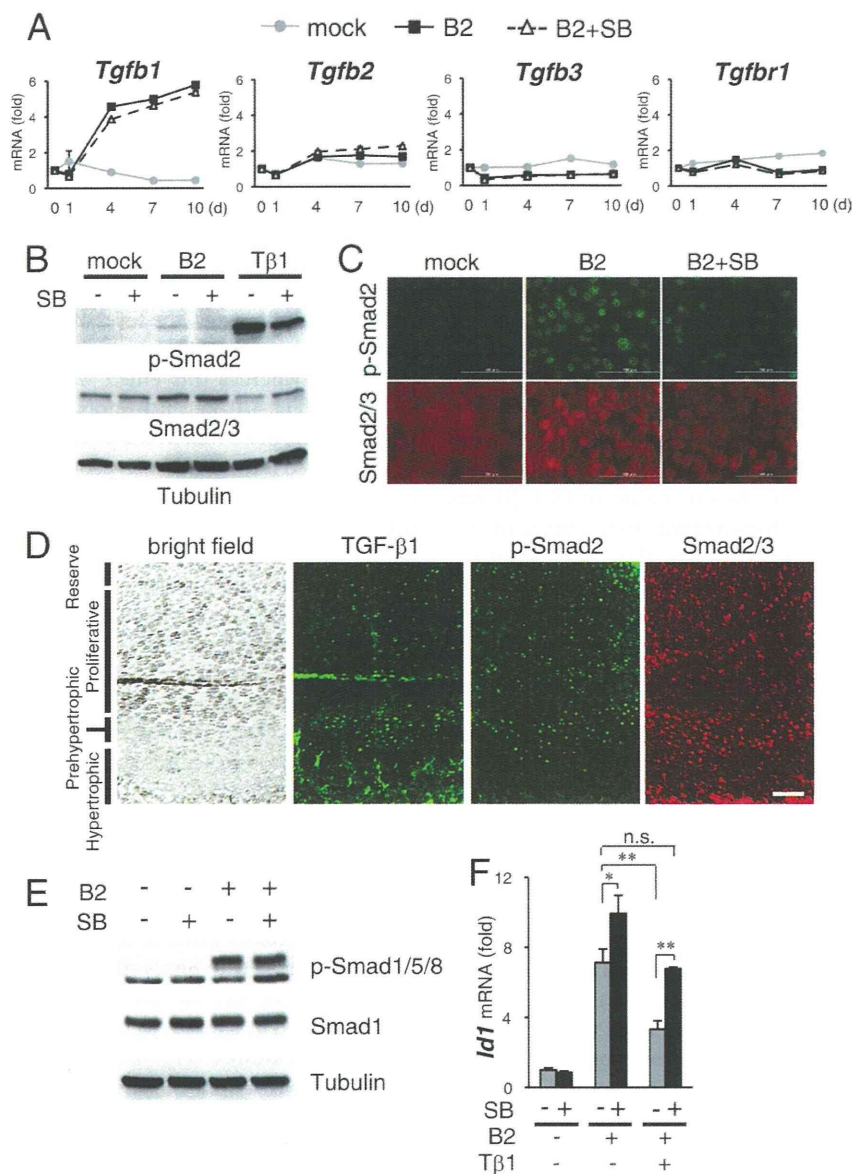
FIGURE 3. **Endogenous TGF-β signaling is activated in maturing chondrocytes to suppress the expression of *Id1*, a direct target gene of BMP-Smad pathway.** *A*, ATDC5 chondrocytes were cultured with BMP-2 (*B2*; 300 ng/ml) in combination with SB431542 (*SB*; 1 μM) for the indicated times. Expression of *Tgfb1*, *Tgfb2*, *Tgfb3*, and *Tgfbr1* were examined by qPCR. *B*, status of TGF-β signaling activity was evaluated by immunoblotting for phosphorylated Smad2 (*p-Smad2*). ATDC5 cells were stimulated with BMP-2 for 7 days or TGF-β1 (*Tβ1*; 5 ng/ml) for 1 h, with or without SB431542. Immunoblot for tubulin served as loading control. *C*, status of TGF-β signaling activity was evaluated by immunocytochemistry for phosphorylated Smad2. ATDC5 cells were stimulated with BMP-2 for 4 days with or without SB431542. *D*, expression of TGF-β1 and status of intracellular TGF-β signaling activity (*p-Smad2*) in mouse E17.5 humerus cartilage were evaluated by immunohistochemistry. *E*, status of BMP signaling activity was evaluated by immunoblotting for phosphorylated Smad1/5/8 (*p-Smad1/5/8*). ATDC5 cells were stimulated with BMP-2 for 4 days, with or without SB431542. Immunoblot for tubulin served as loading control. *F*, expression of *Id1* in ATDC5 cells at day 5 of stimulation was evaluated by qPCR. *Scale bar*, 100 μm. *, *p* < 0.05; **, *p* < 0.01; *n.s.*, not significant. *Error bars*, S.D.

ment (Fig. 2*C*). Moreover, the expression of *Mmp13*, encoding the collagenase matrix metallopeptidase 13 specifically expressed by the terminal hypertrophic chondrocytes, was dramatically up-regulated by blockade of the TGF-β signaling pathway at both mRNA and protein levels (Fig. 2, *D* and *E*). These data demonstrate the cell-autonomous inhibitory action of endogenous TGF-β signaling in the late stage of chondrocyte differentiation.

Endogenous TGF-β Signaling Is Up-regulated during Maturation of Chondrocytes—Because SB431542 affected the late stage of chondrocyte differentiation, we assessed if the expres-

sion of any of the three TGF-β ligands was increased during BMP-induced maturation of ATDC5 chondrocytes. Although the mRNA levels of *Tgfb2* and *Tgfb3* were marginally changed by application of BMP-2 or SB431542, *Tgfb1* (encoding TGF-β1) was dramatically increased from day 4 and further remained up-regulated by BMP-2 treatment, whereas it was not affected by SB431542 (Fig. 3*A*). Because TGF-β ligands transduce the signal through TGF-β type I receptor ALK5, encoded by *Tgfbr1*, we asked if expression of *Tgfbr1* was accelerated in maturing ATDC5 cells. However, the expression level of *Tgfbr1* was unchanged by BMP-2 application (Fig. 3*A*). Therefore, we

evaluated if increased *Tgfb1* expression reflected intracellular signal transduction (Fig. 3*B*). As a positive control, exogenously applied TGF-β1 potently induced the C-terminal phosphorylation of Smad2, which was weakened by SB431542. Importantly, in BMP-2-treated ATDC5 chondrocytes, Smad2 was phosphorylated at a comparatively weak but detectable level, which was suppressed by SB431542 (Fig. 3*B*). In addition, an immunocytochemistry for phosphorylated Smad2 in ATDC5 cells showed that endogenous TGF-β signaling was activated in BMP-2-treated chondrocytes, which was blocked by SB431542 (Fig. 3*C*). These data indicated that the activation of Smad2 by BMP-2 was achieved through the TGF-β type I receptor, probably by the up-regulated production of TGF-β1 in ATDC5 cells. In developing humerus growth plate of E17.5 mouse embryo, moderate expression of TGF-β1 was detected in proliferative chondrocytes, suggesting its role in promoting early chondrogenesis (Fig. 3*D*). Importantly, the expression of TGF-β1 was further accentuated in the prehypertrophic zone and the matrix around the hypertrophic chondrocytes (Fig. 3*D*). Similarly, Smad2 was phosphorylated in some of the proliferative chondrocytes, whereas phospho-Smad2 was detected in most of the prehypertrophic chondrocytes (Fig. 3*D*). Interestingly, Smad2 was not phosphorylated in hypertrophic chondrocytes. These results from immunohistochemistry suggested that expression of TGF-β1 was elevated to up-regulate TGF-β signaling in prehypertrophic chondrocytes, whereas the signaling was inhibited with in hypertrophic chondrocytes, in the endochondral ossification process.

Because Smad3 signaling had been suggested to suppress BMP pathway in maturing chondrocytes (26), we examined immunoblotting for the phosphorylated Smad1/5/8 to investigate the role of endogenous TGF-β signaling against the BMP-Smad signaling system in chondrocytes. BMP-2 induced potent C-terminal phosphorylation of Smad1/5/8 in ATDC5 cells, even at day 4 of induction, whereas combined treatment with SB431542 showed no effect (Fig. 3*E*). However, interestingly, the expression of *Id1*, a specific direct target of the canonical BMP-Smad pathway (33), was significantly elevated by SB431542 treatment, whereas it was suppressed by exogenously applied TGF-β1 (Fig. 3*F*). These data suggest that BMP-induced activation of endogenous TGF-β signaling inhibited BMP signaling downstream of R-Smad activation as a negative feedback mechanism. These data also confirmed that SB431542 is an appropriate tool to screen for putative molecular mediator(s) downstream of endogenous TGF-β signaling to inhibit BMP signaling in chondrocytes.

SnoN Is Induced by Endogenous TGF-β Signaling in Maturing Chondrocytes—The BMP signaling system is negatively regulated at multiple steps (*e.g.* by extracellular antagonists (*e.g.* Noggin, Chordin, Dan, and Cerberus), inhibitory Smads (I-Smads; Smad6 and Smad7), E3 ubiquitin ligases (*e.g.* Smurf1 and Smurf2), and the Ski/SnoN family of transcriptional corepressors) (34, 35). We asked if any of these BMP signaling inhibitors were induced downstream of endogenous TGF-β signaling in maturing chondrocytes. In micromass cultures of ATDC5 chondrocytes, treatment with TGF-β1, as positive control, significantly elevated only the expression of *Smad7* and *SnoN*, both of which are the direct target genes of the TGF-β-

Smad pathway (supplemental Fig. 1). In BMP-2-induced maturing cells, *Smad6*, *Smad7*, and *SnoN* were up-regulated, whereas combined treatment with SB431542 completely inhibited only the elevation of *SnoN* (supplemental Fig. 1). In mouse primary chondrocytes at day 14 of BMP treatment, SnoN was also significantly elevated; this effect was not observed by combined application with SB431542 (Fig. 4*A*). These data indicate that, among the examined BMP inhibitors, SnoN was exclusively induced by the enhanced endogenous TGF-β signaling in maturing chondrocytes. During the maturation phase of ATDC5 chondrocytes, the level of *SnoN* mRNA was increased from days 4 to 10 of BMP application and mildly decreased thereafter, whereas this effect was completely prevented by SB431542 (Fig. 4*B*). Because SnoN is an unstable protein, which has a half-life of 30 min in the presence of TGF-β signaling (36, 37), we asked if the protein level of SnoN reflects the pattern of its mRNA expression and performed an immunoblot for SnoN protein (Fig. 4*C*). As control to identify specific bands for endogenous SnoN protein, we performed a knockdown assay against *SnoN* in monolayer cultures of ATDC5 cells (Fig. 4*C*, *lanes 5–7*). At day 3, the signals of two major bands of around 80 kDa were increased in BMP-2-treated cells, both of which were efficiently abolished by siSnoN, indicating that these bands represented the two isoforms, SnoN and SnoN2 (38). In micromass cultures of ATDC5 chondrocytes at day 7 of BMP-2 application, SnoN protein expression was also induced and further weakened by SB431542 (Fig. 4*C*, *lanes 1–4*), indicating that the expression of the SnoN protein was indeed induced by endogenous TGF-β signaling in maturing chondrocytes. We also confirmed the induction of SnoN protein by immunocytochemistry. Treatment with TGF-β1 for 16 h potently increased the signal of SnoN protein, which was only faintly detected in cells transfected with SnoN siRNA (Fig. 4*D*). At day 4 of BMP-2 stimulation, the level of SnoN protein was up-regulated, which was weakened by siSnoN, in maturing ATDC5 chondrocytes of monolayer cultures (Fig. 4*E*). The knockdown efficiency of SnoN in BMP-2-treated cells was relatively weak, probably because 5 days had passed since the transfection of siRNA. Next, to confirm that the inhibitory effect of SB431542 against the expression level of *SnoN* was exclusive for the late maturation phase, we stimulated ATDC5 cells with BMP-2 in combination with SB431542 and harvested the cells at the early time points within 36 h of induction (Fig. 4*F*). To our surprise, *SnoN* was rapidly induced by BMP-2 after 1 h and was decreased to reach the basal level thereafter, an expression pattern that was similar to that of *Id1* (Fig. 4*F*). However, this transient induction of *SnoN* by BMP-2 was not affected by SB431542, suggesting that endogenous TGF-β signaling was not responsible for this up-regulation of *SnoN*.

To investigate the possibility that SnoN plays a role in chondrogenesis *in vivo*, its expression in cartilage tissue was examined. We extracted RNA from various tissues of 3-month-old adult mice to prepare tissue panels of cDNA to analyze the tissue distribution. Consistent with the report that heterozygous *SnoN* knock-out mice developed T lymphomas in the spleen, which indicates an important role of SnoN in the spleen (39), we detected the highest level of *SnoN* expression in the spleen (Fig. 4*G*). Interestingly, the comparatively highest level
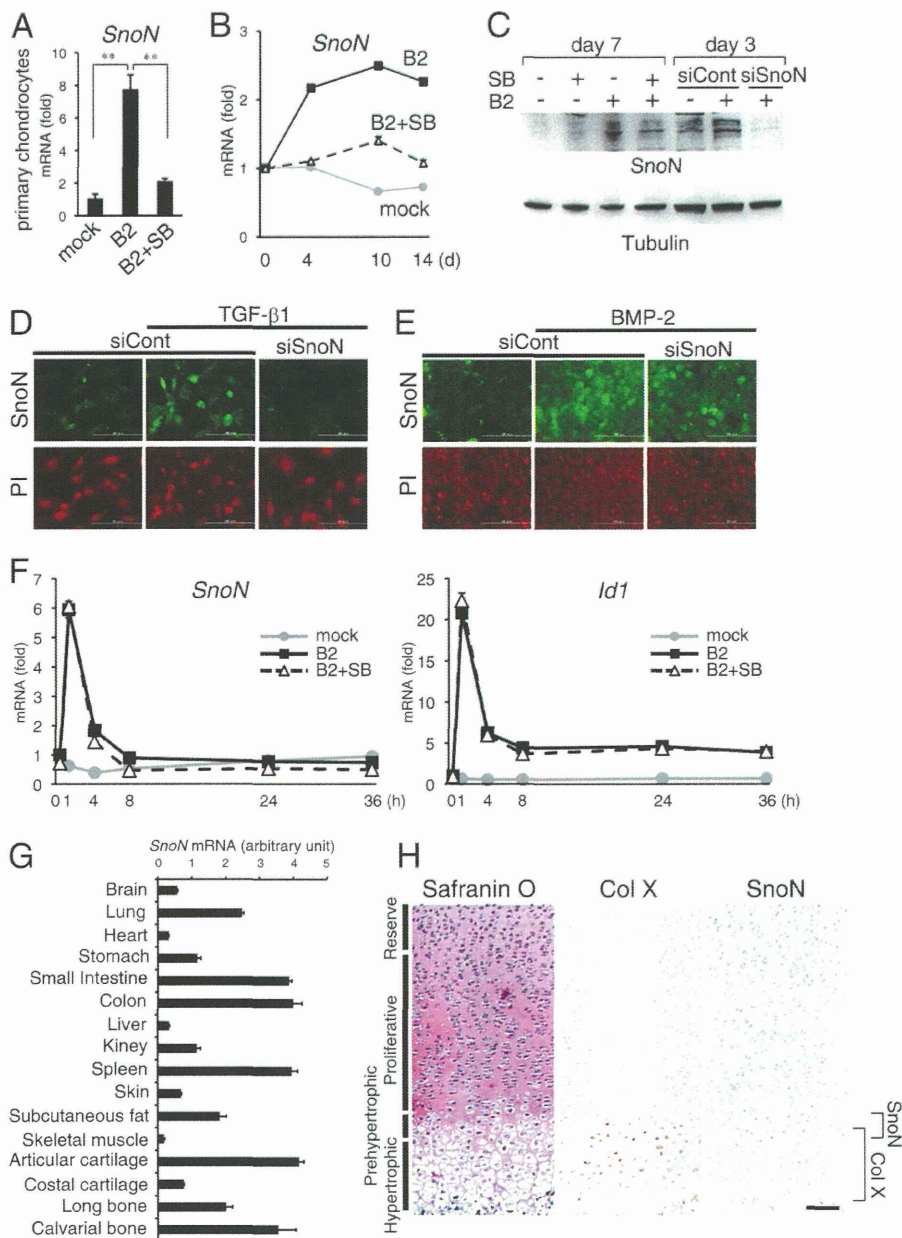
FIGURE 4. SnoN is induced in maturing chondrocytes by endogenous TGF-β signaling *in vitro*, whereas it is highly expressed in cartilage tissue in mice. *A,* expression of *SnoN* in primary chondrocytes at day 14 of stimulation was evaluated by real-time RT-PCR. Cells were stimulated with BMP-2 (*B2;* 300 ng/ml) with or without SB431542 (*SB;* 1 μM). *B,* ATDC5 chondrocytes were cultured with or without SB431542 for the indicated times, after which the samples were subjected to qPCR analysis for *SnoN. C,* expression of SnoN protein in ATDC5 cells was assessed by immunoblotting. Differentiation of ATDC5 cells was induced by incubation with BMP-2 for 7 days (*lanes 1–4*). As a control, cells were transfected with siSnoN for 16 h and further cultured in the presence of BMP-2 for 3 days (*lanes 5–7*). Tubulin served as a loading control. *D* and *E,* immunocytochemistry for SnoN was performed on a monolayer culture of ATDC5 cells. Cells were transfected with siRNA for 16 h and further incubated with or without TGF-β1 (5 ng/ml) for 16 h (*D*) or with or without BMP-2 for 4 days (*E*). MG132 (10 μM) was applied 16 h prior to cell fixation. Nuclei were visualized with propidium iodide (*PI*). *Scale bars,* 100 μm. *F,* ATDC5 chondrocytes were stimulated with BMP-2 in combination with SB431542 for the indicated time points. cDNA samples were subjected to qPCR analysis for *SnoN* and *Id1. G,* tissue cDNA panel of 3-month-old mice was subjected to real-time PCR for *SnoN. H,* protein expression of type X collagen (*Col X*) and SnoN in E17.5 humerus cartilage was determined by immunohistochemistry. Zones of positive signal were indicated. Proteoglycans in cartilage matrix were stained by Safranin O. *Scale bar,* 100 μm. **, $p < 0.01$. *Error bars,* S.D.

of *SnoN* expression was found in articular cartilage (Fig. 4*G*). Immunohistochemistry for the growth plate of developing bone of mouse embryos at E17.5, in which endochondral ossification was in progress, detected the signal of type X collagen protein from the lower half of prehypertrophic chondrocytes to the entire area of hypertrophic chondrocytes (Fig. 4*H*). Impor-

tantly, although SnoN protein was detected weakly in proliferating chondrocytes, its potent signal was present in prehypertrophic chondrocytes, whereas it was weakened in hypertrophic chondrocytes (Fig. 4*H*). These data suggest that SnoN is highly expressed in premature chondrocytes before hypertrophic conversion, *in vitro* and *in vivo*.
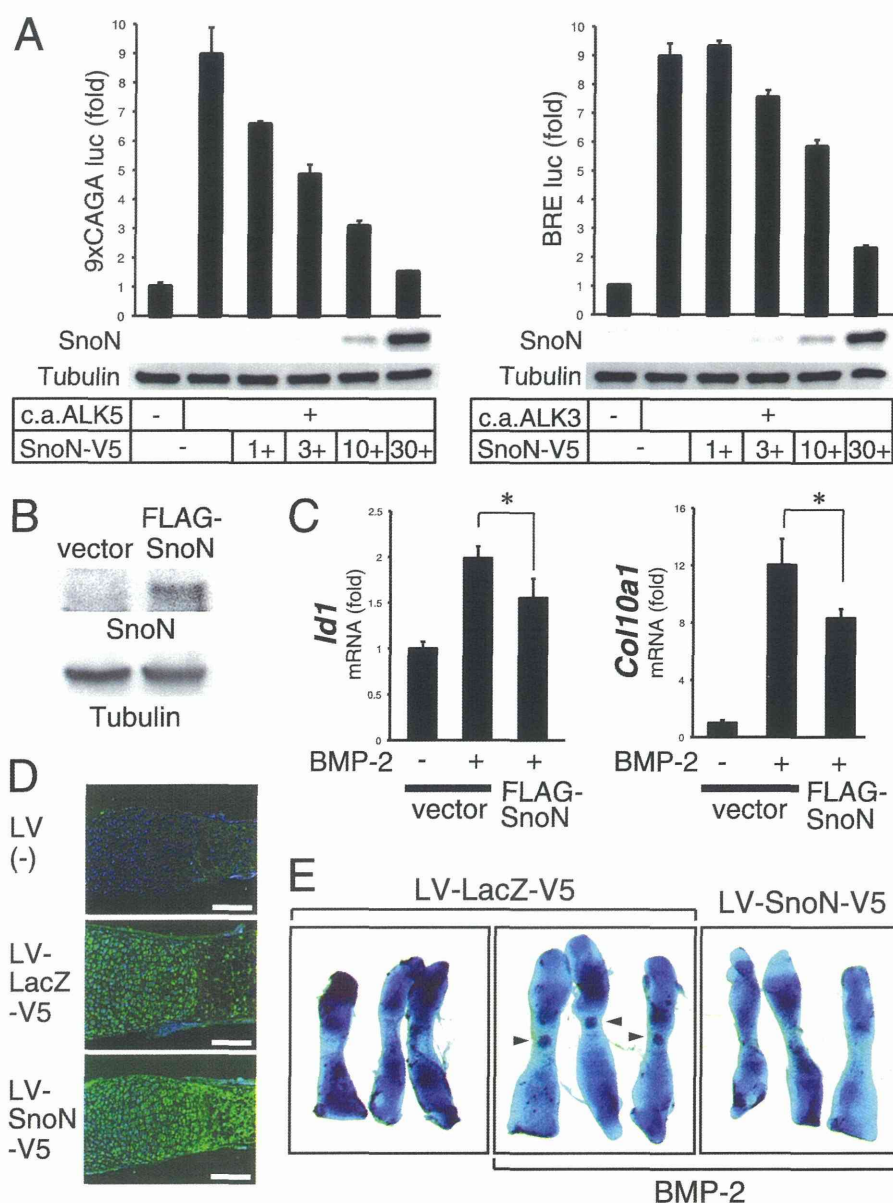
FIGURE 5. **SnoN suppresses BMP signaling and subsequent chondrocyte maturation.** *A*, SnoN expression vector was transfected with plasmids of constitutively active type I receptors and a luciferase reporter of 9xCAGA luc (for TGF-β signaling) or BRE luc (for BMP signaling) into COS-7 cells. Expression of transfected SnoN was confirmed by anti-SnoN immunoblot. Tubulin served as loading control. *B*, FLAG-tagged SnoN expression vector was stably transfected into ATDC5 chondrocytes, and its expression was confirmed by anti-SnoN immunoblotting. *C*, SnoN suppressed expression of *Id1* as well as *Col10a1* at day 7 of BMP-2 (300 ng/ml) treatment in a stable transfectant of ATDC5 chondrocytes. *D* and *E*, metatarsal bones of E17.5 mouse embryo were infected with indicated lentivirus (*LV*) for 16 h. Immunostaining using FITC-linked anti-V5 antibody on bone coronal sections was performed at day 2 of culture to evaluate the efficiency of lentiviral infection. Nuclei were stained with Hoechst dye. Merged images are presented. LV-LacZ-V5 served as a lentiviral infection control (*D*). *Scale bars*, 200 μm. Alcian blue/alizarin red staining was performed at day 2 of BMP-2 treatment (*E*). The *arrowheads* indicate the calcified cartilage matrix in bone rudiments of triplicate culture. *, $p < 0.05$. *Error bars*, S.D.

SnoN Suppresses the BMP-Smad Signaling Pathway to Inhibit Hypertrophic Maturation of Chondrocytes—SnoN interacts with Smad2, Smad3, and Smad4 in the cytoplasm to prevent their nuclear translocation (40, 41). In the nucleus, it represses their transcriptional activity by disrupting the active trimeric Smad complex and recruiting transcriptional corepressors (36), thereby negatively regulating TGF-β signaling. It is not known whether SnoN suppresses canonical BMP-Smad signaling in the same manner as the related family molecule

c-Ski (42); however, SnoN may inhibit the pathway because of its ability to bind Smad4, although it cannot bind Smad1/5/8 (43). To test this hypothesis, SnoN was investigated using a BRE luciferase reporter specifically responding to the BMP-Smad pathway (33) in COS-7 cells. As a positive control for the SnoN function, SnoN was applied to the 9xCAGA TGF-β signal reporter (44), activated by constitutively active TGF-β type I receptor ALK5, to show a dose-dependent potent inhibition (Fig. 5*A*, *left*). Interestingly, SnoN did suppress the activity of
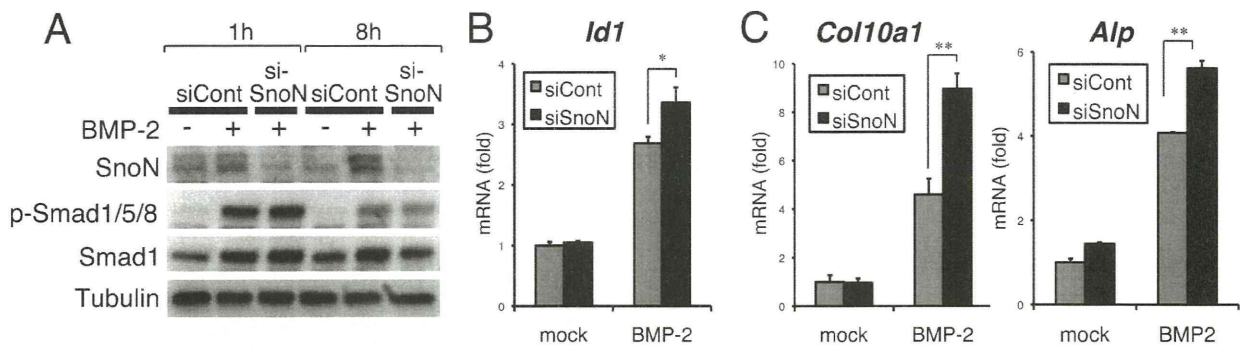
FIGURE 6. Loss of SnoN in ATDC5 chondrocytes mimics the effect of SB431542, which accelerates the expression of *Id1* and hypertrophic marker genes. *A*, ATDC5 cells were stimulated by BMP-2 (300 ng/ml) 16 h after transfection with siRNA. Cells harvested at the indicated time points were subjected to immunoblotting. *B* and *C*, ATDC5 chondrocytes were transfected with siRNA for 16 h, followed by induction of differentiation with BMP-2 for 3 days. Expression of *Id1*, *Col10a1*, and *Alp* was analyzed by real-time RT-PCR. *, $p < 0.05$; **, $p < 0.01$. *Error bars*, S.D.

the BRE reporter induced by the constitutively active type I BMP receptor ALK3 (encoded by *Bmpr1a*) (Fig. 5*A*, *right*) in a dose-dependent manner, although more than 3 times the amount of SnoN plasmid DNA was required for the inhibition compared with the reporter assay using 9xCAGA. Next, we stably transfected a FLAG-tagged SnoN expression vector into ATDC5 cells and confirmed the transgene expression by anti-SnoN immunoblotting (Fig. 5*B*). In ATDC5 chondrocytes, gain of SnoN suppressed the elevated expression of *Id1* at day 7 of BMP-2 induction (Fig. 5*C*, *left*). The increased expression of the hypertrophic marker *Col10a1* was also down-regulated by SnoN in BMP-treated ATDC5 cells (Fig. 5*C*, *right*). Thus, forced expression of SnoN in ATDC5 chondrocytes inhibited BMP signaling and, subsequently, chondrocyte maturation. To investigate the role of SnoN in cartilage maturation, we infected lentivirus carrying V5-tagged SnoN expression cassette into E17.5 metatarsal bone rudiments. We confirmed the infection efficiency of the lentivirus by performing immunohistochemistry on the coronal sections of the bones, using anti-V5-FITC antibody to detect the transgene product (Fig. 5*D*). In lentivirus-infected bones, we found the certain expression of V5-tagged transgenes in the cells of perichondrium and the chondrocytes in zones of reserve, proliferative, and prehypertrophic but not hypertrophic chondrocytes. Treatment of BMP-2 induced calcification of the hypertrophic zone of bone rudiments (Fig. 5*E*, *arrowheads*), whereas overexpression of SnoN by lentivirus completely prevented the cartilage mineralization (Fig. 5*E*). These data demonstrate that gain of SnoN inhibits the maturation of the hypertrophic chondrocytes.

Next, we investigated the physiological role of endogenous SnoN in ATDC5 chondrocytes by performing an siRNA-mediated knockdown assay. We confirmed that SnoN protein expression was induced upon BMP-2 induction, even at the early time points, and that the two bands (representing SnoN and SnoN2) could be efficiently eliminated by siSnoN (Fig. 6*A*). BMP-2 induced a potent phosphorylation of Smad1/5/8, whereas siSnoN showed no effect on the phosphorylation level, even after the phosphorylation declined at 8 h (Fig. 6*A*). However, knockdown of SnoN mildly, but significantly, enhanced the BMP-2-induced increase of the *Id1* gene at day 4 in ATDC5 cells (Fig. 6*B*). siSnoN further significantly enhanced the BMP-induced up-regulation of *Col10a1* as well as alkaline phospha-

tase (*Alp*), another marker of matured hypertrophic chondrocytes (Fig. 6*C*). These data for the SB431542-mimicking effects of siSnoN (Figs. 2 and 3) indicated that SnoN mediated a major part of the roles of endogenous TGF-β signaling in chondrocytes to physiologically suppress BMP signaling and subsequent chondrocyte hypertrophic maturation without affecting the activating step of Smad1/5/8.

TGF-β Signaling and Expression of SnoN Are Accentuated in "Prehypertrophic" Chondrocytes Adjacent to Pathologically Hypertrophic Chondrocyte in Moderately Affected OA Cartilage—Given the role of SnoN in the prevention of hypertrophic conversion of chondrocytes, SnoN protein may be present before pathologic chondrocytes gained hypertrophic phenotype in OA cartilages (8, 9). We performed immunohistochemistry assays for SnoN in human OA cartilages of various severities. In normal adult human femoral head cartilage, expression of type X collagen was entirely absent, whereas SnoN protein was weakly detected in the superficial zone (Fig. 7*A*). In moderate OA cartilage, in which the severity was graded as 6 according to the modified Mankin score (45, 46), type X collagen-positive pathologically hypertrophic chondrocytes were located in the upper layer of degenerated cartilage, which was poorly stained by Safranin O. Strikingly, we detected potent signals for SnoN protein in chondrocytes in which the cell body was mildly enlarged, resembling "prehypertrophic" chondrocytes in the developing bone. These SnoN-positive cells formed colonies located in close proximity of the colonies of hypertrophic chondrocytes (Fig. 7*A*). In severe OA cartilage of a grading score of 10, the cartilage surface of which was entirely destroyed, a few colonies of pathologically hypertrophic chondrocytes expressing type X collagen were present; however, we could no longer detect SnoN-positive cells (Fig. 7*A*). These data are consistent with our hypothesis that SnoN prevents the progression of hypertrophic conversion of articular chondrocytes. Finally, we asked if this enhanced expression of SnoN protein was associated with TGF-β signaling in human OA cartilage, similarly as observed in the growth plate of mouse embryo (Figs. 3*D* and 4*H*). In moderate OA cartilage, an immunofluorescence assay revealed the abundant accumulation of TGF-β1 protein around the "prehypertrophic" chondrocytes (Fig. 7*B*). Moreover, phosphorylated active Smad3 was detected in these pathologic chondrocytes. Again, SnoN protein was also expressed in chon-
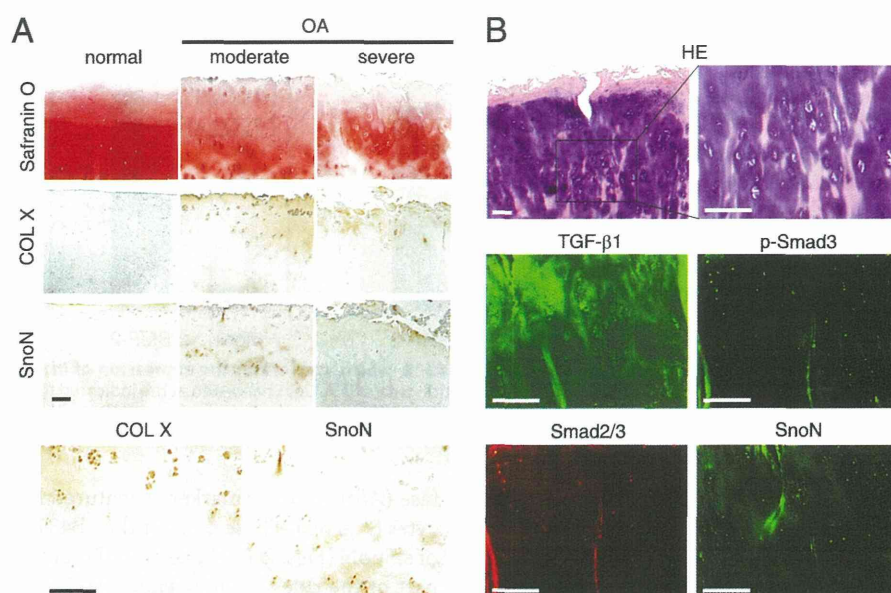
FIGURE 7. TGF-β signaling and expression of SnoN are up-regulated in mildly hypertrophic chondrocytes located adjacent to colonies of pathologically hypertrophic chondrocytes in human OA cartilage. *A,* human OA cartilage samples were subjected to immunohistochemistry for type X collagen (*COL X*) and SnoN. The severity of OA was graded according to the modified Mankin score on the basis of the histology of cartilage specimens stained with Safranin O. *Bottom panel,* magnified images of a moderate OA sample in the *top panel. B,* the human OA cartilage specimen of moderate severity was subjected to hematoxylin and eosin (*HE*) staining and immunohistochemistry for TGF-β1, phosphorylated Smad3 (*p-Smad3*), total Smad2/3, and SnoN. *Scale bars,* 200 µm.

drocytes in this region. These data demonstrated an association of TGF-β signaling and expression of SnoN in the degenerating cartilage.

DISCUSSION

Endogenous TGF-β Signaling Is Activated in Maturing Chondrocytes to Induce SnoN—Although the importance of TGF-β signaling in preventing hypertrophic conversion of chondrocytes has been demonstrated (23, 24, 47), the mode of TGF-β signaling during chondrocyte maturation and its direct target gene(s) responsible for inhibiting the differentiation remain largely unknown. While exogenously applied TGF-β has been reported to have a positive role in early chondrogenesis *in vitro,* SB431542 showed no effect on bone growth, whereas it dramatically enhanced the matrix calcification by the mature hypertrophic chondrocytes in a bone organ culture system (Fig. 1). This result suggested that endogenous TGF-β signaling was more active in the late stage of maturing chondrocytes than in the early stage of chondrocyte differentiation. Indeed, expression of *Tgfb1* was up-regulated in the late phase of differentiation of ATDC5 chondrocytes (Fig. 3*A*), coupled with an increase in phosphorylation of Smad2, which was inhibited by SB431542 (Fig. 3, *B* and *C*). This was completely linked to the expression pattern of SnoN (Fig. 4, *A–C*). SnoN expression was probably directly induced by endogenous TGF-β signaling because *SnoN* had been shown to be directly induced by TGF-β-activated Smad2 through its binding to the Smad-binding element in the promoter of the *SnoN* gene (48). Interestingly, in Smad3-deficient chondrocytes, the expression of TGF-β1, TGF-β type I receptor ALK5 (*Tgfbr1*), and SnoN was suppressed, whereas the expression of Smad1, Smad5, Smad6, BMP-2, and BMP-6 was elevated (26), suggesting SnoN to be one of the downstream targets of TGF-β signaling in chondro-

cytes. For the first time, we demonstrated the rapid and transient induction of *SnoN* by exogenously applied BMP ligand, whereas it was not suppressed by SB431542 (Fig. 4*F*). The *SnoN* expression pattern in the early phase, which resembled that of *Id1* (Fig. 4*F*), led us to hypothesize that the BMP-Smad pathway, in addition to TGF-β-Smad signaling, can directly induce *SnoN* in a context-dependent manner. Indeed, the sequences of GGCACC or GGCGCG, both of which contain a 1-base mismatch with the BMP-Smad-responsive motif GGCGCC (33), can be found adjacent to three TGF-β-responsive CAGA Smad-binding elements in the *SnoN* promoter (48). Further experiments are required to resolve this hypothesis and to evaluate the roles of BMP-Smad-induced SnoN.

SnoN Interferes with BMP Signaling to Suppress Hypertrophic Differentiation of Chondrocytes—The *Sno* gene (whose name derived from "*Ski*-related <u>no</u>vel gene") was initially discovered on the basis of its close homology to v-Ski and c-Ski. Ski proteins can suppress TGF-β signaling, as well as BMP signaling, by binding to R-Smads and Smad4. Interestingly, although c-Ski can interact weakly with Smad1/5, the strong interaction with Smad4 is indispensable for suppression of BMP signaling by c-Ski (42). Although SnoN interacts with Smad4, the role of SnoN in the context of BMP signaling has not been well investigated. We showed here that SnoN suppressed BMP signaling in a comparative but slightly weaker manner compared with TGF-β signaling (Fig. 5*A*). This weaker suppression of BMP signaling is probably due to the difference in the accessibility to Smads (*i.e.* SnoN could bind to Smad2/3 and Smad4 but not to Smad1/5, unlike c-Ski) (43). Loss of SnoN mildly enhanced the expression of *Id1,* whereas it did not affect the phosphorylation level of Smad1/5/8 (Fig. 6, *A* and *B*), supporting the notion that the functional molecular target of SnoN was not the phosphor-

ylation step of Smad1/5/8 but rather Smad4. Because siSnoN and SB431542 showed an essentially similar effect with regard to phospho-Smad1/5/8 and *Id1* expression (compare Fig. 3, *E* and *F*, and Fig. 6, *A* and *B*), SnoN seems to be one of the major mediators of TGF-β signaling to inhibit BMP signaling in chondrocytes. This is interesting because we previously reported a similar negative feedback mechanism regulated by signal crosstalk between TGF-β and BMP signaling in osteoblast differentiation, in which I-Smads were induced by endogenous TGF-β signaling to inhibit BMP signaling in the maturation phase (49). However, the expression of I-Smads was not dramatically affected by SB431542 in ATDC5 chondrocytes (supplemental Fig. 1), suggesting context-dependent mechanisms in the selection of TGF-β target genes in these mesenchymal cells. The effect of forced expression, or knockdown, of SnoN showed more dramatic changes in the *Col10a1* expression than in that of *Id1* (Figs. 5*C* and 6*C*). The persistently mild suppression of BMP signaling by SnoN during the maturing phase may account for the major inhibition of hypertrophic maturation of chondrocytes.

Expression of SnoN Is Associated with the Enhanced TGF-β Signaling in Prehypertrophic Chondrocytes in Mouse Developing Bone and Human OA Cartilage—Maintenance of the articular cartilage depends on the function of articular chondrocytes, which produce cartilage matrix and are constrained from undergoing the maturation program seen in growth plate chondrocytes of developing bone. Genetic association of single nucleotide polymorphisms (SNPs) in the *SMAD3* or *ASPN* gene (encoding asporin) with human OA has been reported (50, 51). Asporin was shown to bind TGF-β ligands on the cell surface to block their signal transduction (52). In articular cartilage of old mice, decreased expression of TGF-β ligands and receptors, coupled with strongly dropped phosphorylation of Smad2, was observed (53). Moreover, as mentioned in the Introduction, mouse models of loss of TGF-β signaling showed an OA phenotype with accelerated hypertrophic conversion of chondrocytes. These lines of evidence clearly demonstrate the importance of TGF-β signaling in preventing OA change of articular chondrocytes. To date, the mechanism by which TGF-β signaling regulates this process is largely unknown. One candidate for targeting TGF-β signaling is Smurf2, a protein whose expression was up-regulated in human OA cartilage, whereas forced expression of Smurf2 in chondrocytes developed OA change in joints of the transgenic mice (25). Because Smurf2 is a TGF-β-inducible molecule to inhibit TGF-β signaling, it may mediate the effect of TGF-β signaling in chondrocyte hypertrophy. However, in *Smad3*-deficient chondrocytes, which showed enhanced BMP signaling and accelerated maturation, expression of *Smurf2* was not affected (26). Similarly, in our ATDC5 micromass culture system, *Smurf2* was not elevated in maturing ATDC5 chondrocytes stimulated by BMP-2 (supplemental Fig. 1). In contrast, we detected an increase of SnoN expression, not only in both maturing ATDC5 cells and primary chondrocytes *in vitro* but also in prehypertrophic chondrocytes in mouse developing bone and in human OA cartilage (Figs. 4 and 7). Although we demonstrated the inhibitory role of SnoN in chondrocyte hypertrophy *in vitro* (Figs. 5 and 6), hypertrophy of chondrocytes was present in both developing normal mouse

cartilage and degenerating human OA cartilage, despite the accentuated expression of SnoN in contiguous prehypertrophic chondrocytes (Figs. 4*H* and 7). In mouse E17.5 bone, phosphorylation of Smad2 and expression of SnoN were diminished in hypertrophic chondrocytes despite the abundant accumulation of TGF-β1 protein in the extracellular matrix (Figs. 3*D* and 4*H*), suggesting a disorder of the signal transduction by unknown mechanisms to be resolved. Similarly, in human OA cartilage, expression of SnoN was weakened in colonies of COL X-positive hypertrophic cells (Fig. 7*A*). Taken together, it is likely that the hypertrophic conversion was induced after the decline of SnoN expression in these chondrocytes. In this regard, further investigation is required to understand why the transduction of TGF-β signaling and subsequent expression of SnoN are diminished in hypertrophic chondrocytes. Although our results do not establish an etiologic role for SnoN in the progression of OA, they at least establish a strong association that explains a possible causal relationship between SnoN regulation and hypertrophic conversion of chondrocytes in OA cartilage. Loss of SnoN in mice *in vivo* should reveal its putative roles in cartilage hypertrophy or endochondral ossification; however, SnoN knock-out mice showed embryonic lethality at E3.5 (39). Therefore, a conditional knock-out mouse line of chondrocyte-specific ablation of the *SnoN* gene would be suitable to address these questions. In conclusion, our data revealed a novel role of SnoN in regulating BMP signaling and subsequent chondrocyte maturation as a downstream mediator of TGF-β signaling. SnoN may be targeted in chondrocytes to inhibit its function in order to accelerate endochondral ossification or to enhance its activity in the case of treating OA or cartilage regeneration for repair.

REFERENCES

1. Akiyama, H., Chaboissier, M. C., Martin, J. F., Schedl, A., and de Crombrugghe, B. (2002) The transcription factor Sox9 has essential roles in successive steps of the chondrocyte differentiation pathway and is required for expression of Sox5 and Sox6. *Genes Dev.* **16**, 2813–2828
2. Provot, S., and Schipani, E. (2005) Molecular mechanisms of endochondral bone development. *Biochem. Biophys. Res. Commun.* **328**, 658–665
3. Enomoto, H., Enomoto-Iwamoto, M., Iwamoto, M., Nomura, S., Himeno, M., Kitamura, Y., Kishimoto, T., and Komori, T. (2000) Cbfa1 is a positive regulatory factor in chondrocyte maturation. *J. Biol. Chem.* **275**, 8695–8702
4. Zheng, Q., Zhou, G., Morello, R., Chen, Y., Garcia-Rojas, X., and Lee, B. (2003) Type X collagen gene regulation by Runx2 contributes directly to its hypertrophic chondrocyte-specific expression *in vivo. J. Cell Biol.* **162**, 833–842
5. Ueta, C., Iwamoto, M., Kanatani, N., Yoshida, C., Liu, Y., Enomoto-Iwamoto, M., Ohmori, T., Enomoto, H., Nakata, K., Takada, K., Kurisu, K., and Komori, T. (2001) Skeletal malformations caused by overexpression of Cbfa1 or its dominant negative form in chondrocytes. *J. Cell Biol.* **153**, 87–100
6. Takeda, S., Bonnamy, J. P., Owen, M. J., Ducy, P., and Karsenty, G. (2001) Continuous expression of Cbfa1 in nonhypertrophic chondrocytes uncovers its ability to induce hypertrophic chondrocyte differentiation and partially rescues Cbfa1-deficient mice. *Genes Dev.* **15**, 467–481
7. Scotti, C., Tonnarelli, B., Papadimitropoulos, A., Scherberich, A., Schaeren, S., Schauerte, A., Lopez-Rios, J., Zeller, R., Barbero, A., and Martin, I.

(2010) Recapitulation of endochondral bone formation using human adult mesenchymal stem cells as a paradigm for developmental engineering. *Proc. Natl. Acad. Sci. U.S.A.* **107**, 7251–7256

8. Pullig, O., Weseloh, G., Ronneberger, D., Käkönen, S., and Swoboda, B. (2000) Chondrocyte differentiation in human osteoarthritis. Expression of osteocalcin in normal and osteoarthritic cartilage and bone. *Calcif. Tissue Int.* **67**, 230–240

9. Sandell, L. J., and Aigner, T. (2001) Articular cartilage and changes in arthritis. An introduction. Cell biology of osteoarthritis. *Arthritis Res.* **3**, 107–113

10. Dreier, R. (2010) Hypertrophic differentiation of chondrocytes in osteoarthritis. The developmental aspect of degenerative joint disorders. *Arthritis Res. Ther.* **12**, 216

11. Nelea, V., Luo, L., Demers, C. N., Antoniou, J., Petit, A., Lerouge, S., R Wertheimer, M., and Mwale, F. (2005) Selective inhibition of type X collagen expression in human mesenchymal stem cell differentiation on polymer substrates surface-modified by glow discharge plasma. *J. Biomed. Mater. Res. A* **75**, 216–223

12. Sekiya, I., Vuoristo, J. T., Larson, B. L., and Prockop, D. J. (2002) *In vitro* cartilage formation by human adult stem cells from bone marrow stroma defines the sequence of cellular and molecular events during chondrogenesis. *Proc. Natl. Acad. Sci. U.S.A.* **99**, 4397–4402

13. Miyazono, K., Kamiya, Y., and Morikawa, M. (2010) Bone morphogenetic protein receptors and signal transduction. *J. Biochem.* **147**, 35–51

14. Tsumaki, N., Nakase, T., Miyaji, T., Kakiuchi, M., Kimura, T., Ochi, T., and Yoshikawa, H. (2002) Bone morphogenetic protein signals are required for cartilage formation and differently regulate joint development during skeletogenesis. *J. Bone Miner. Res.* **17**, 898–906

15. Yoon, B. S., Ovchinnikov, D. A., Yoshii, I., Mishina, Y., Behringer, R. R., and Lyons, K. M. (2005) Bmpr1a and Bmpr1b have overlapping functions and are essential for chondrogenesis *in vivo. Proc. Natl. Acad. Sci. U.S.A.* **102**, 5062–5067

16. Retting, K. N., Song, B., Yoon, B. S., and Lyons, K. M. (2009) BMP canonical Smad signaling through Smad1 and Smad5 is required for endochondral bone formation. *Development* **136**, 1093–1104

17. Furumatsu, T., Tsuda, M., Taniguchi, N., Tajima, Y., and Asahara, H. (2005) Smad3 induces chondrogenesis through the activation of SOX9 via CREB-binding protein/p300 recruitment. *J. Biol. Chem.* **280**, 8343–8350

18. Volk, S. W., Luvalle, P., Leask, T., and Leboy, P. S. (1998) A BMP-responsive transcriptional region in the chicken type X collagen gene. *J. Bone Miner. Res.* **13**, 1521–1529

19. Leboy, P., Grasso-Knight, G., D'Angelo, M., Volk, S. W., Lian, J. V., Drissi, H., Stein, G. S., and Adams, S. L. (2001) Smad-Runx interactions during chondrocyte maturation. *J. Bone Joint Surg. Am.* **83-A**, Suppl. 1, S15–S22

20. Kempf, H., Ionescu, A., Udager, A. M., and Lassar, A. B. (2007) Prochondrogenic signals induce a competence for Runx2 to activate hypertrophic chondrocyte gene expression. *Dev. Dyn.* **236**, 1954–1962

21. Kobayashi, T., Lyons, K. M., McMahon, A. P., and Kronenberg, H. M. (2005) BMP signaling stimulates cellular differentiation at multiple steps during cartilage development. *Proc. Natl. Acad. Sci. U.S.A.* **102**, 18023–18027

22. van Beuningen, H. M., Glansbeek, H. L., van der Kraan, P. M., and van den Berg, W. B. (1998) Differential effects of local application of BMP-2 or TGF-β1 on both articular cartilage composition and osteophyte formation. *Osteoarthr. Cartil.* **6**, 306–317

23. Yang, X., Chen, L., Xu, X., Li, C., Huang, C., and Deng, C. X. (2001) TGF-β/Smad3 signals repress chondrocyte hypertrophic differentiation and are required for maintaining articular cartilage. *J. Cell Biol.* **153**, 35–46

24. Serra, R., Johnson, M., Filvaroff, E. H., LaBorde, J., Sheehan, D. M., Derynck, R., and Moses, H. L. (1997) Expression of a truncated, kinase-defective TGF-β type II receptor in mouse skeletal tissue promotes terminal chondrocyte differentiation and osteoarthritis. *J. Cell Biol.* **139**, 541–552

25. Wu, Q., Kim, K. O., Sampson, E. R., Chen, D., Awad, H., O'Brien, T., Puzas, J. E., Drissi, H., Schwarz, E. M., O'Keefe, R. J., Zuscik, M. J., and Rosier, R. N. (2008) Induction of an osteoarthritis-like phenotype and degrada-

tion of phosphorylated Smad3 by Smurf2 in transgenic mice. *Arthritis Rheum.* **58**, 3132–3144

26. Li, T. F., Darowish, M., Zuscik, M. J., Chen, D., Schwarz, E. M., Rosier, R. N., Drissi, H., and O'Keefe, R. J. (2006) Smad3-deficient chondrocytes have enhanced BMP signaling and accelerated differentiation. *J. Bone Miner. Res.* **21**, 4–16

27. Bobick, B. E., and Kulyk, W. M. (2004) The MEK-ERK signaling pathway is a negative regulator of cartilage-specific gene expression in embryonic limb mesenchyme. *J. Biol. Chem.* **279**, 4588–4595

28. Gosset, M., Berenbaum, F., Thirion, S., and Jacques, C. (2008) Primary culture and phenotyping of murine chondrocytes. *Nat. Protoc.* **3**, 1253–1260

29. Alvarez, J., Sohn, P., Zeng, X., Doetschman, T., Robbins, D. J., and Serra, R. (2002) TGFβ2 mediates the effects of hedgehog on hypertrophic differentiation and PTHrP expression. *Development* **129**, 1913–1924

30. Tominaga, H., Maeda, S., Hayashi, M., Takeda, S., Akira, S., Komiya, S., Nakamura, T., Akiyama, H., and Imamura, T. (2008) CCAAT/enhancer-binding protein β promotes osteoblast differentiation by enhancing Runx2 activity with ATF4. *Mol. Biol. Cell* **19**, 5373–5386

31. Ahrens, P. B., Solursh, M., and Reiter, R. S. (1977) Stage-related capacity for limb chondrogenesis in cell culture. *Dev. Biol.* **60**, 69–82

32. Shukunami, C., Ohta, Y., Sakuda, M., and Hiraki, Y. (1998) Sequential progression of the differentiation program by bone morphogenetic protein-2 in chondrogenic cell line ATDC5. *Exp. Cell Res.* **241**, 1–11

33. Korchynskyi, O., and ten Dijke, P. (2002) Identification and functional characterization of distinct critically important bone morphogenetic protein-specific response elements in the Id1 promoter. *J. Biol. Chem.* **277**, 4883–4891

34. Canalis, E., Economides, A. N., and Gazzerro, E. (2003) Bone morphogenetic proteins, their antagonists, and the skeleton. *Endocr. Rev.* **24**, 218–235

35. Miyazono, K., Maeda, S., and Imamura, T. (2005) BMP receptor signaling. Transcriptional targets, regulation of signals, and signaling cross-talk. *Cytokine Growth Factor Rev.* **16**, 251–263

36. Stroschein, S. L., Wang, W., Zhou, S., Zhou, Q., and Luo, K. (1999) Negative feedback regulation of TGF-β signaling by the SnoN oncoprotein. *Science* **286**, 771–774

37. Sun, Y., Liu, X., Ng-Eaton, E., Lodish, H. F., and Weinberg, R. A. (1999) SnoN and Ski protooncoproteins are rapidly degraded in response to transforming growth factor β signaling. *Proc. Natl. Acad. Sci. U.S.A.* **96**, 12442–12447

38. Pearson-White, S., and Crittenden, R. (1997) Proto-oncogene Sno expression, alternative isoforms and immediate early serum response. *Nucleic Acids Res.* **25**, 2930–2937

39. Shinagawa, T., Dong, H. D., Xu, M., Maekawa, T., and Ishii, S. (2000) The *sno* gene, which encodes a component of the histone deacetylase complex, acts as a tumor suppressor in mice. *EMBO J.* **19**, 2280–2291

40. Jahchan, N. S., You, Y. H., Muller, W. J., and Luo, K. (2010) Transforming growth factor-β regulator SnoN modulates mammary gland branching morphogenesis, postlactational involution, and mammary tumorigenesis. *Cancer Res.* **70**, 4204–4213

41. Krakowski, A. R., Laboureau, J., Mauviel, A., Bissell, M. J., and Luo, K. (2005) Cytoplasmic SnoN in normal tissues and nonmalignant cells antagonizes TGF-β signaling by sequestration of the Smad proteins. *Proc. Natl. Acad. Sci. U.S.A.* **102**, 12437–12442

42. Takeda, M., Mizuide, M., Oka, M., Watabe, T., Inoue, H., Suzuki, H., Fujita, T., Imamura, T., Miyazono, K., and Miyazawa, K. (2004) Interaction with Smad4 is indispensable for suppression of BMP signaling by c-Ski. *Mol. Biol. Cell* **15**, 963–972

43. Wang, W., Mariani, F. V., Harland, R. M., and Luo, K. (2000) Ski represses bone morphogenic protein signaling in *Xenopus* and mammalian cells. *Proc. Natl. Acad. Sci. U.S.A.* **97**, 14394–14399

44. Dennler, S., Itoh, S., Vivien, D., ten Dijke, P., Huet, S., and Gauthier, J. M. (1998) Direct binding of Smad3 and Smad4 to critical TGF β-inducible elements in the promoter of human plasminogen activator inhibitor-type 1 gene. *EMBO J.* **17**, 3091–3100

45. Mankin, H. J., Dorfman, H., Lippiello, L., and Zarins, A. (1971) Biochemical and metabolic abnormalities in articular cartilage from osteo-arthritic